Central European Journal of Energetic Materials
ISSN 1733-7178; e-ISSN 2353-1843

Cent. Eur. J. Energ. Mater. 2017, *14*(2): 336-350 DOI: 10.22211/cejem/68475

Synthesis of Hexabenzylhexaazaisowurtzitane (HBIW) under Ultrasound Irradiation with Fe_3O_4@PCA Nanoparticles as an Efficient and Reusable Nanomagnetic Catalyst

Asemeh Mashhadi Malekzadeh,[1] **Sahar Shokrollahi,**[1] **Ali Ramazani,**[1*] **Seyed Jamal Tabatabaei Rezaei,**[1] **Pegah Azimzadeh Asiabi,**[1] **Sang Woo Joo**[2**]

[1] *Department of Chemistry, University of Zanjan, PO Box 45195-313, Zanjan, Iran*
[2] *School of Mechanical Engineering, Yeungnam University, Gyeongsan 712-749, Republic of Korea*
*E-mail: *aliramazani@gmail.com*, **swjoo@yu.ac.kr*

Abstract: Magnetic Fe_3O_4@polycitric acid (Fe_3O_4@PCA) nanoparticles were prepared by the reaction of Fe_3O_4 nanoparticles with an excess amount of citric acid at 100-160 °C. The magnetic Fe_3O_4@PCA nanoparticles were characterized by infrared spectroscopy (FTIR), scanning electron microscope (SEM), Transmission Electron Microscopy (TEM), Thermogravimetric Analysis (TGA) and powder X-ray diffraction (XRD). Finally, the synthesized magnetic Fe_3O_4@PCA nanoparticles were used as a heterogeneous solid acid catalyst for the synthesis of HBIW from benzylamine and glyoxal in acetonitrile-water solvent under ultrasonic irradiation conditions. The catalyst could be reused up to 6 times without significant loss of activity.

Keywords: hexabenzylhexaazaisowurtzitane (HBIW), nanomagnetic catalyst, solid acid, Fe_3O_4@PCA, ultrasound irradiation

1 Introduction

Nanotechnology has been one of the most active research areas in recent years [1]. Magnetic nanoparticles (MNPs) are a class of nanostructured materials. On this

basis, MNPs have many unique magnetic properties such as superparamagnetism, high coercivity, low Curie temperature and high magnetic susceptibility. MNPs are of great interest for researchers because of their potential biomedical applications in fields such as drug delivery [2, 3], magnetic resonance imaging [4], biomolecular sensors [5] and bioseparation [6]. Among the various magnetic nanoparticles, Fe_3O_4 nanoparticles (NPs) are the most extensively studied. The main characteristics of these nanoparticles are their good stability, easy synthesis and functionalization, high surface area and facile separation by magnetic forces, as well as low toxicity and price [7, 8]. Additionally, recent studies show that MNPs are excellent catalysts for organic reactions [9-11]. Also, surface modification of MNPs is a general and graceful way to bridge the gap between heterogeneous and homogeneous systems. These attractive features have made MNPs a promising alternative to porous/mesoporous catalyst supports. Thus, the development of coated MNPs for supporting catalysts is currently a subject of increasing interest in chemical processing [12, 13].

Since, the defense industry is a model for development in various industries, a possible way to promote this progress consists of designing highly energetic compounds that provide explosive power superior to any existing substance [14-16]. Cage crystal molecules containing nitro groups are important and widely used as high energetic materials and have attracted much attention in the last ten years [17-19]. According to theoretical predictions of their physicochemical and explosion characteristics, polycyclic nitramines, in particular, hexanitrohexaazaisowurtzitane, HNIW (or CL-20), is a unique representative of this class of compounds [20, 21]. Hexabenzylhexaazaisowurtzitane (HBIW) is used as a precursor for the synthesis of HNIW. The only available method for the construction of the HBIW cage is based on the condensation of glyoxal with benzylamine in the presence of formic acid as catalyst [22]. Although this method is efficient, catalyst recovery/reuse is not possible. Therefore, the discovery of new and inexpensive catalysts for the preparation of HBIW under mild conditions is of prime importance.

Ultrasound irradiation is an efficient and safe technique for the synthesis of inorganic and organic compounds. In comparison to the classical methods, this method leads to chemical reactions under milder reaction conditions, higher yields and shorter reaction times [23-29]. The aim of this work was the study of polycitric acid supported on Fe_3O_4 NPs (Fe_3O_4@PCA) with inherent magnetic properties as a novel catalyst for the development of a new eco-compatible synthetic strategy.

Therefore, we wished to explore a straightforward synthesis of 2,4,6,8,10,12-hexabenzyl-2,4,6,8,10,12-hexaazatetracyclo[5,5,0,$0^{5,9}$,$0^{3,11}$]

dodecane (HBIW) using Fe_3O_4@PCA as a proficient, mild, environmentally friendly, recyclable, low toxicity and magnetic powerful solid acid catalyst with good stability under ultrasound irradiation conditions (Scheme 1).

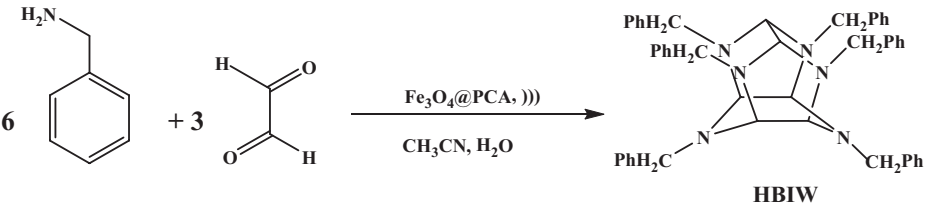

Scheme 1. Preparation of HBIW catalyzed by Fe_3O_4@PCT

2 Materials and Methods

2.1 Apparatus, materials and measurements

All high purity chemicals, including iron(III) chloride anhydrous ($FeCl_3$), iron(II) sulfate heptahydrate ($FeSO_4 \cdot 7H_2O$), benzylamine, glyoxal, citric acid monohydrate, acetonitrile, ethanol, methanol, chloroform, dichloromethane, tetrahydrofuran, 25% ammonia solution (NH_3) were purchased from Fluka and Merck (Darmstadt, Germany). Melting points were determined using an Electrothermal 9100 apparatus. The structural properties of Fe_3O_4@PCA MNPs were analyzed by X-ray powder diffraction (XRD) with an X'Pert-PRO advanced diffractometer using Cu Kα radiation (wavelength: 1.5406 Å), operated at 40 kV and 40 MA at room temperature in the range of 2θ from 20° to 80°. The particle size and morphology of the surfaces of the sample were analyzed using a scanning electron microscope (KYKY Co., China, Model: EM 3200). Infrared spectra were recorded with a Mattson (Unicam Ltd., Cambridge, UK) 1000 Fourier transform infrared spectrophotometer using the KBr technique. ^{1}H NMR and ^{13}C NMR spectra ($CDCl_3$) were recorded on a Bruker (Karlsruhe, Germany) DRX-250 Avance spectrometer at 250.0 MHz. Sonication was performed in a Bandelin (Berlin, Germany) SONOPULS ultrasonic homogenizer at a processing frequency of 20 kHz, a nominal power of 250 W, and uniform sound waves. The amount of grafted PCA to the magnetic nanoparticles was determined using a Thermogravimetric Analyzer (TGA Q500) up to 800 °C in air at a ramp rate of 10 K·min^{-1}. The size and morphological characterization of the magnetic nanoparticles were carried out using a Zeiss-EM10C Transmission Electron Microscope (TEM) operating at 80 kV. TEM samples were prepared by dispersing the magnetic nanoparticles in deionized water for 30 min by ultrasonic

irradiation. The aqueous dispersion was dropped onto a carbon coated copper TEM grid (300 Mesh) with filter paper underneath to absorb the deionized water and dried in vacuum.

2.2 Synthesis of Fe_3O_4 MNPs

Magnetite nanoparticles were prepared through a coprecipitation method according to a previously reported procedure [30] with only a slight change. Briefly, $FeSO_4 \cdot 7H_2O$ and $FeCl_3$ were dissolved in water in 1:2 molar ratios under nitrogen protection. The resulting dark orange solution was stirred for 10 min at 80 °C. An aqueous NH_3 solution (1.5 M) was then added dropwise to the hot solution while stirring over a period of 15 min. An instant color change from dark orange to black was found to occur when the particles formed. Stirring was then continued for a further 30 min followed by cooling to room temperature. The solvent was removed by magnetic decantation. Washing of the particles with water and then ethanol was performed several times to make the iron dispersion free of any residual salts. The dispersion was then used during the coprecipitation. The final supernatant was decanted magnetically to obtain the as-prepared superparamagnetic iron oxide NPs.

2.3 Synthesis of Fe_3O_4 @ PCA

MNPs (0.1 g) were added to a polymerization ampule equipped with a magnetic stirrer and vacuum inlet. Monohydrate citric acid (1 g) was added to the ampule which was then sealed under vacuum. The mixture was heated up to 120 °C and stirred at this temperature for 30 min. After removing the water by vacuum inlet, the reaction temperature was raised to 140 °C and stirred at this temperature for 1 h. Again the water produced was removed by vacuum inlet and the reaction temperature was raised to 160 °C. Polymerization was continued at this temperature under dynamic vacuum (open vacuum inlet) for 1.5 h. The coated nanoparticles were purified by using a permanent magnet and then washed first with THF and then with ethyl acetate. They were then dried for characterization. The attachment of PCA to the iron oxide nanoparticles was confirmed by FTIR analysis and the samples dried under vacuum before analysis.

2.4 Typical procedure for synthesis of HBIW

Benzylamine (0.0085 mol, 0.937 mL), Fe_3O_4@PCT (5 wt.% with respect to glyoxal), acetonitrile (7.75 mL), and water (0.775 mL) were placed in a round-bottomed 100 mL flask. The reaction mixture was stirred at room temperature and glyoxal (40% aqueous solution; 0.00375 mol, 0.427 mL) was added dropwise (15 min). Then the mixture was irradiated with ultrasound for 5 min under

a power of 150 W. The formation of HBIW was monitored by TLC.

After satisfactory completion of the reaction, the reaction mixture was washed with cold excess ethanol and the catalyst removed using a magnetic field. The solid residue was isolated and purified by recrystallization in acetonitrile.

2.5 Physical and spectral data of the product

White solid; m.p.: 154-157 °C. FT-IR (KBr) (ν_{max}/cm^{-1}): 3022, 2942, 2835, 1951, 1601, 1450, 1351, 1169, 1138, 989, 926, 836, 732, 699. ^{1}H NMR ($CDCl_3$) δ_H: 7.24-7.28 (m, 30H, phenyl CH), 4.16 (s, 4H, CH_2), 4.09 (s, 8H, CH_2), 4.04 (s, 4H, CH), 3.57 (s, 2H, CH). ^{13}C NMR ($CDCl_3$): 56.21 (4C, CH_2-phenyl), 56.9 (2C, CH_2-phenyl) 76.9 (4C, CH (skeletal)), 80.64 (2C, CH (skeletal)), 126.62-140.74 (36C, phenyl).

3 Results and Discussion

Fe_3O_4@PCA core-shell nanoparticles, with Fe_3O_4 spheres as the core and polycitric acid (PCA) as the shell, were prepared by a simple, low cost and convenient method. Magnetite nanoparticles were synthesized by the co-precipitation of $FeSO_4 \cdot 7H_2O$ and $FeCl_3$ in aqueous ammonia solution. To improve the chemical stability of MNPs, their surface engineering was successfully performed by the suitable deposition of polycitric acid (PCA) onto the surface of the nanoparticles by polymerization of citric acid (Scheme 2). A proposed mechanism for the synthesis of HBIW catalyzed by Fe_3O_4@PCT is presented in Scheme 3.

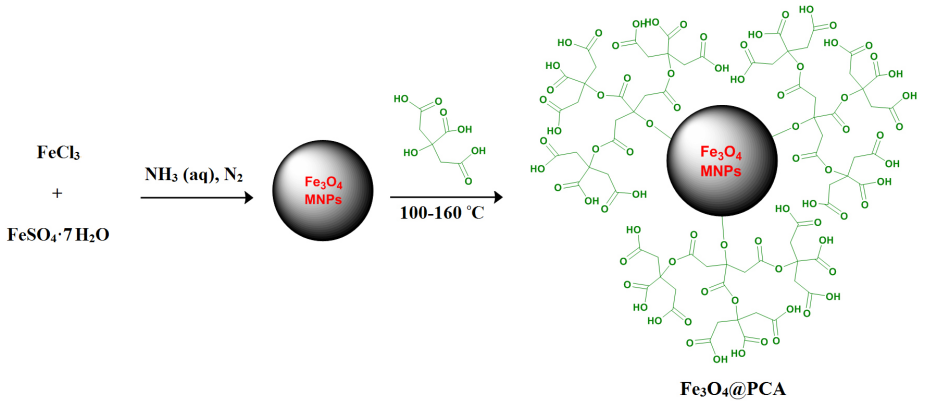

Scheme 2. Schematic diagram for the synthesis of Fe_3O_4@PCA

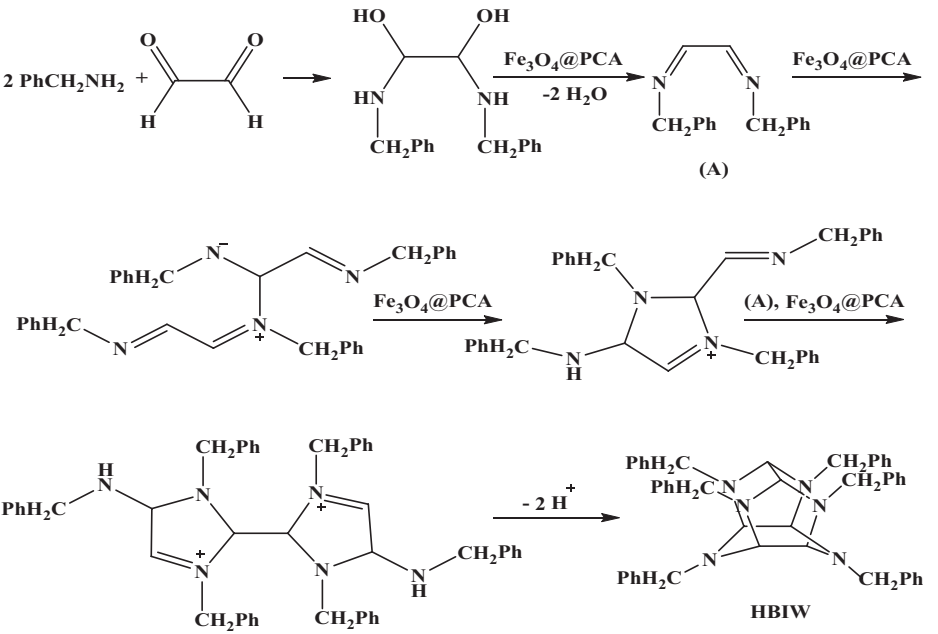

Scheme 3. A proposed mechanism for the synthesis of HBIW in the presence of Fe_3O_4@PCA

The Fe_3O_4@PCA nanoparticles were characterized by FT-IR, SEM, TEM, TGA and XRD. To demonstrate the successful synthesis of Fe_3O_4@PCA, FT-IR was carried out, and Figure 1 represented the FT-IR spectrum of Fe_3O_4 and Fe_3O_4@PCA. In Figure 1, the peak at about 564 cm^{-1} was due to the vibration of Fe–O bonds. In Figure 1b, the peaks in the range 3050-3630 cm^{-1} were attributed to the hydroxyl functional groups of the grafted PCA. In these spectra, the absorbance band of the carbonyl groups of citric acid appeared in the range 1502-1722 cm^{-1} and the peaks in the range 1255-1443 cm^{-1} were due to the C–O in Fe_3O_4@PCA [31].

The structure of Fe_3O_4 and Fe_3O_4@PCA were analyzed by X-ray powder diffraction (XRD). The XRD pattern of the Fe_3O_4@PCA (Figure 2b) showed all the major peaks corresponding to Fe_3O_4. The $2\theta = 30.1°$, 35.6°, 43.1°, 53.2°, 57.2° and 62.9° can be assigned to the (220), (311), (400), (422), (511) and (440) planes, respectively. Attachment of PCA to the surface of Fe_3O_4 nanoparticles causes the broadening of the XRD peaks. The broadening of the XRD peaks of Fe_3O_4 may result from the effects of PCA grafted on the surface of Fe_3O_4 that also were observed in previous reports [32, 33]. This result confirmed successful surface modification of the Fe_3O_4 NPs.

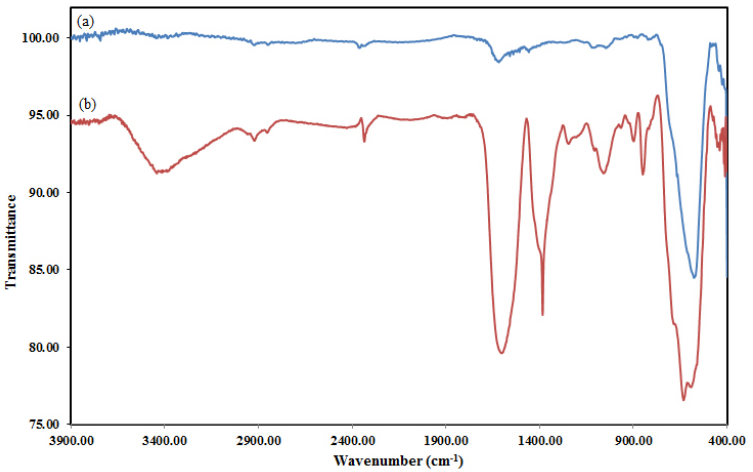

Figure 1. FT-IR spectrum of Fe_3O_4 (a), Fe_3O_4@ PCA (b)

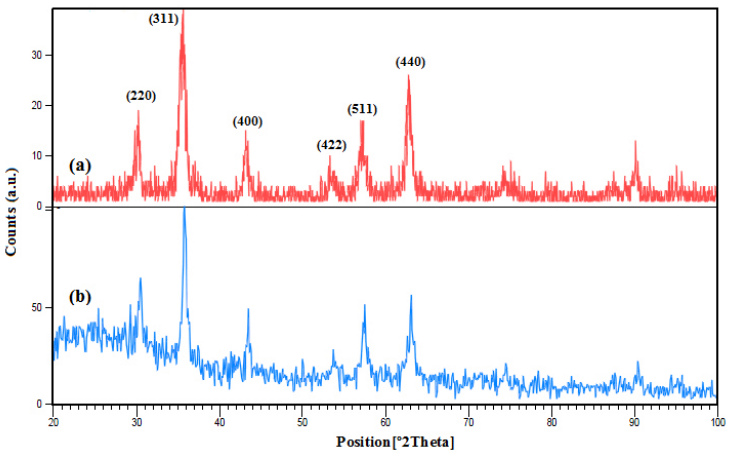

Figure 2. XRD pattern of Fe_3O_4 (a), Fe_3O_4@PCA (b)

The morphology and size of the magnetic nanoparticles have been known to be affected by several factors, including the reaction conditions and chemicals involved. Figure 3 shows an SEM image of Fe_3O_4@PCA and it could be observed that all the nanoparticles have a regular spherical shape with an average particle diameter in the range of 40.3 nm.

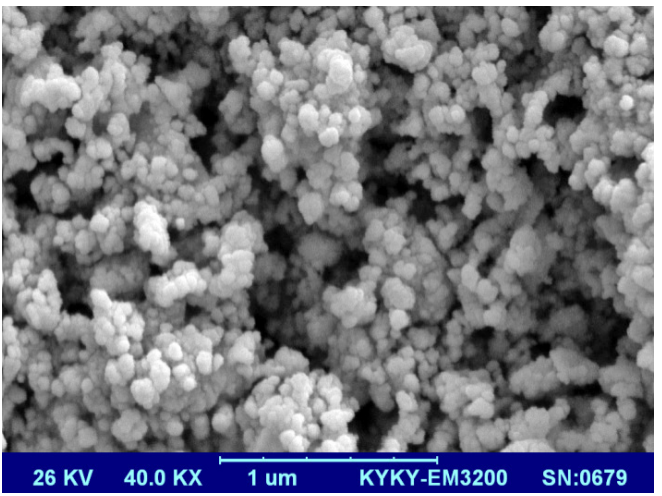

Figure 3. SEM micrograph of Fe_3O_4@PCA

The grafted polycitric acid content of the MNPs can be calculated using the TGA method (Figure 4). Figure 4 curve (a0 shows that the weight loss of bare MNPs over the temperature range from 20 °C to 800 °C is about 4.4% which resulted from the loss of residual water in the sample. In Fe_3O_4@PCA, the weight loss is about 20.9% which reflects the amount of grafted PCA on the surface of the magnetic nanoparticles (Figure 4 curve (b)) [34].

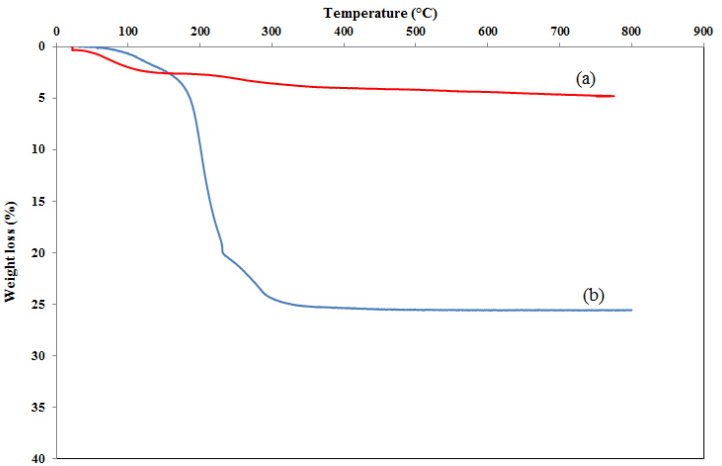

Figure 4. TGA curves of Fe_3O_4 (a), Fe_3O_4@ CA (b)

The morphologies and particle sizes of the prepared nanoparticles were investigated using TEM on their suspensions. Figure 6 shows a TEM image of Fe_3O_4@PCA and it can be observed that all the nanoparticles have a regular spherical shape with an average particle diameter in the range of 10-20 nm that show the nanoparticles have a core-shell structure. The particle sizes of the Fe_3O_4@PCA measured using SEM (Figure 3) were greater than the corresponding TEM results. This difference is due to differences in the the sample preparation methods for analysis and instrumentation mechanism. SEM analysis is a useful method for understanding surface morphology and gives particles sizes with a low resolution, precision and accuracy. In the TEM we can usually say whether each particle is an agglomerate composed of smaller crystallites (average crystallite size = X) or whether each particle is a single crystallite. And finally, when we present SEMs of fracture surfaces of our bulk samples, we definitely make references to average grain size. So it is very normal that the TEM results give lower particle sizes in comparison with the corresponding SEM results.

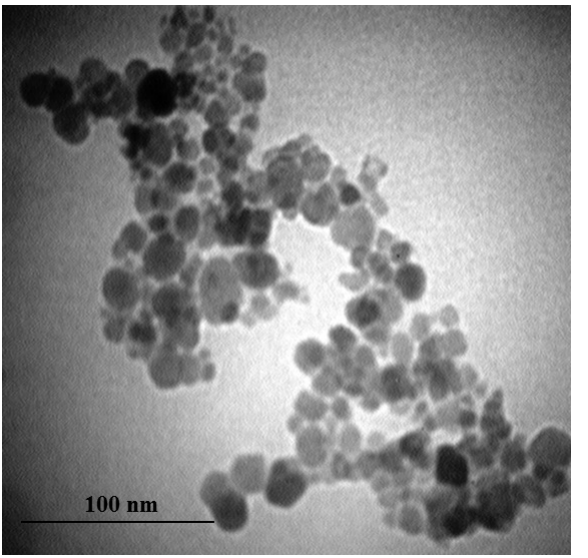

Figure 6. TEM micrograph of Fe_3O_4@PCA

After characterization of the Fe_3O_4@PCA catalyst, we tested its catalytic activity in the preparation of HBIW.

3.1 Effect of catalyst amount on product yield

In order to verify the effect of catalyst amount on product yield, the reaction between benzylamine and glyoxal was performed in the presence of various amounts of catalyst in acetonitrile (Table 1). The results clearly show that the product yield increased with increasing amounts of catalyst up to 5 wt.%. However, in the absence of catalyst, the reaction yielded only 17% of the product.

Table 1. Effect of the catalyst in the synthesis of HBIW [a]

Entry	Catalyst	Content [wt.%]	Time [min]	Yield [b] [%]
1	No catalyst	-	5	17
2	Formic acid	10	15	51
3	Fe_3O_4	5	5	48
4	Citric acid	5	5	89
5	Fe_3O_4@PCT	1	5	66
6	Fe_3O_4@PCT	3	5	77
7	Fe_3O_4@PCT	5	5	91
8	Fe_3O_4@PCT	10	5	92
9	Fe_3O_4@PCT	15	5	92

[a] Reaction conditions: benzylamine (0.0085 mol, 0.937 mL), glyoxal (0.0037 mol, 0.427 mL), CH_3CN (7.75 mL), H_2O (0.775 mL), and catalyst (wt.% with respect to glyoxal) at room temperature and ultrasonic power of 150 W.
[b] Yields of isolated products.

3.2 Effect of solvent on the product yield

The results are summarized in Table 2. It is seen that when ethanol, chloroform, dichloromethane and tetrahydrofuran were chosen as the reaction medium the yield of product is moderate, while the use of acetonitrile increased the yield of the reaction to 91% and decreased the reaction time to 30 min (Table 2, entry 1). Thus, acetonitrile is suitable for this reaction under ultrasound irradiation. According to the proposed mechanism (Scheme 3), the reaction intermediates are ionic compounds and therefore the process is very sensitive to the solvent polarity. Polar solvents could stabilize the polar reaction transition state better in comparison with less polar solvents. As presented in Table 2, the reaction yield is fairly high in polar solvents by comparison with less polar solvents.

Table 2. Model reaction catalyzed by Fe_3O_4@PCT in different solvents [a]

Entry	Solvent	Yield [b] [%]
1	Acetonitrile	91
2	Ethanol	67
3	Methanol	63
4	Chloroform	64
5	Dichloromethane	54
6	Tetrahydrofuran	58

[a] Reaction conditions: benzylamine (0.0085 mol, 0.937 mL), glyoxal (0.0037 mol, 0.427 mL), solvent (7.75 mL), H_2O (0.775 mL), and Fe_3O_4@PCT (5 wt.% with respect to glyoxal) at room temperature and ultrasonic power of 150 W.
[b] Yields of isolated products.

3.3 Influence of reaction time on the product yield

Since the amount of catalyst and solvent were optimized, the influence of reaction time on the reaction was studied in the next step. The effect of reaction time on the synthesis of HBIW was examined and the results are reported in the Table 3.

Table 3. Different runs for choosing the optimum duration [a]

Entry	Time [min]	Yield [b] [%]
1	3	67
2	5	91
3	10	91
4	15	92
5	30	92

[a] Reaction conditions: benzylamine (0.0085 mol, 0.937 mL), glyoxal (0.0037 mol, 0.427 mL), acetonitrile (7.75 mL), H_2O (0.775 mL), and Fe_3O_4@PCT (5 wt.% with respect to glyoxal) at room temperature and ultrasonic power of 150 W for various times.
[b] Yields of isolated products.

3.4 Influence of ultrasound power on the product yield

In order to verify the effect of irradiation power, the reaction was also performed at 50 W, 100 W, 150 W, and 200 W. By increasing the irradiation power from 50 W to 150 W, the yield increased from 65% to 91% (Table 4). The best yield for HBIW was obtained by ultrasonic irradiation at 150 W for 5 min at room temperature.

Table 4. Effect of ultrasonic irradiation power on the synthesis of HBIW[a]

Entry	Power [W]	Time [min]	Yield[b] [%]
1	50	5	65
2	100	5	75
3	150	5	91
4	200	5	91

[a] Reaction conditions: benzylamine (0.0085 mol, 0.937 mL), glyoxal (0.0037 mol, 0.427 mL), acetonitrile (7.75 mL), H_2O (0.775 mL), and Fe_3O_4@PCT (5 wt.% with respect to glyoxal) at room temperature and ultrasonic different power for 5 min.
[b] Yields of isolated products.

The possibility of magnetic recycling of the catalyst was also examined. In this procedure, after completion of the reaction, ethanol was added and the catalyst was easily separated from the product by attaching an external magnet onto the reaction vessel, followed decantation of the reaction solution. The remaining catalyst was washed with ethyl acetate to remove the residual product and dried under vacuum and reused in a subsequent reaction. The average chemical yield for six consecutive runs was 88%, which clearly demonstrates the practical recyclability of this catalyst (Figure 4).

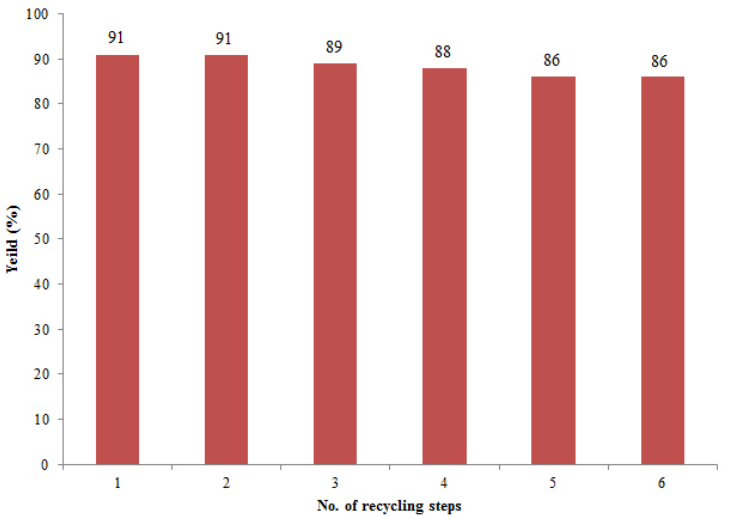

Figure 4. Recyclability of Fe_3O_4@PCA

From the above results, the best reaction conditions for the prepation of HBIW were found to be as follows: benzylamine (0.0085 mol, 0.937 mL),

glyoxal (0.0037 mol, 0.427 mL), Fe_3O_4@PCT (5 wt.% with respect to glyoxal), acetonitrile (7.75 mL), H_2O (0.775 mL), ultrasonic irradiation power (150 W) and room temperature. Under these reaction conditions, HBIW was obtained at high yield (91%) in 5 min.

4 Conclusion

In this research, Fe_3O_4@PCA core-shell nanoparticles were successfully prepared and characterized by FT-IR, SEM and XRD. The catalytic activity of solid acid nanoparticles was probed through the synthesis of hexabenzylhexaazaisowurtzitane (HBIW) under ultrasonic irradiation conditions. The attractive features of this method are: simple procedure, improved yields, cleaner reaction, use of reusable catalyst, simple workup and very short reaction times, making it a useful and environmentally green catalyst.

Acknowledgements
This work is funded by the grant NRF-2015-002423 of the National Research Foundation of Korea.

References

[1] LaConte, L.; Nitin, N.; Bao, G. Magnetic nanoparticle probes. *Mater. Today*. **2005**, *8*: 32-38.
[2] Zhu, Y.; Fang, Y.; Kaskel, S. Folate-Conjugated Fe_3O_4@SiO_2 Hollow Mesoporous Spheres for Targeted Anticancer Drug Delivery. *J. Phys. Chem. C.* **2010**, *114*: 16382-16388.
[3] Fathi, M.; Entezami, A. A.; Arami, S.; Rashidi, M. R. Preparation of N-Isopropylacrylamide/Itaconic Acid Magnetic Nanohydrogels by Modified Starch as a Crosslinker for Anticancer Drug Carriers. *Inter. J. Poly. Mater. Poly. Biomater*. **2015**, *64*: 541-549.
[4] Cui, X.; Belo, S.; Kruger, D.; Yan, Y.; de Rosales, R. T.; Jauregui-Osoro, M.; Blower, P. J. Aluminium Hydroxide Stabilised $MnFe_2O_4$ and Fe_3O_4 Nanoparticles as Dualmodality Contrasts Agent for MRI and PET Imaging. *Biomaterials* **2014**, *35*: 5840-5846.
[5] Graham, D. L.; Ferreira, H. A.; Freitas, P. P. Magnetoresistive-based Biosensors and Biochips. *Trends Biotechnol.* **2004**, *22*: 455-462.
[6] Wang, D.; He, J.; Rosenzweig, N.; Rosenzweig, Z. Superparamagnetic Fe_2O_3 Beads-CdSe/ZnS Quantum Dots Core-Shell Nanocomposite Particles for Cell

Separation. *Nano Lett.* **2004**, *4*: 409-413.
[7] Wei, Y.; Han, B.; Hu, X.; Lin, Y.; Wang, X.; Deng, X. Synthesis of Fe_3O_4 Nanoparticles and Their Magnetic Properties. *Procedia Eng.* **2012**, *27*: 632-637.
[8] El Ghandoor, H.; Zidan, H. M.; Khalil, M. H.; Ismail, M. I. M. Synthesis and Some Physical Properties of Magnetite (Fe_3O_4) Nanoparticles. *Int. J. Electrochem. Sci.* **2012**, *7*: 5734-5745.
[9] Safari, J.; Zarnegar, Z.; Heydarian, M. Magnetic Fe_3O_4 Nanoparticles as Efficient and Reusable Catalyst for the Green Synthesis of 2-Amino-4H-chromene in Aqueous Media. *B. Chem. Soc. Jpn.* **2012**, *85*: 1332-1338.
[10] Zhang, Z.-H.; Lü, H.-Y.; Yang, S.-H.; Gao, J.-W. Synthesis of 2,3-Dihydroquinazolin-4(1*H*)-ones by Three-component Coupling of Isatoic Anhydride, Amines, and Aldehydes Catalyzed by Magnetic Fe_3O_4 Nanoparticles in Water. *J. Comb. Chem.* **2010**, *12*: 643-646.
[11] Senapati, K. K.; Borgohain, C.; Phukan, P. Synthesis of Highly Stable $CoFe_2O_4$ Nanoparticles and Their Use as Magnetically Separable Catalyst for Knoevenagel Reaction in Aqueous Medium. *J. Mol. Catal A- Chem.* **2011**, *339*: 24-31.
[12] Lin, Y.; Chen, H.; Lin, K.; Chen, B.; Chiou, C. Application of Magnetic Particles Modified with Amino Groups to Adsorb Copper Ions in Aqueous Solution. *J. Environ. Sci.* **2011**, *23*: 44-50.
[13] Mahmoodi, N. M.; Khorramfar, S.; Najafi, F. Amine-functionalized Silica Nanoparticle: Preparation, Characterization and Anionic Dye Removal Ability. *Desalination* **2011**, *279*: 61-68.
[14] Andrews, D. H. The Relation between the Raman Spectra and the Structure of Organic Molecules. *Phys. Rev*. **1990**, *36*: 544-554.
[15] Zhou, G.; Wang, J.; He, W.-D.; Wong, N.-B.; Tian, A.; Li, W.-K. Theoretical Investigation of Four Conformations of HNIW by B3LYP Method. *J. Mol. Struct*. **2002**, 589: 273-280.
[16] Yi, W.-B.; Cai, C. Synthesis of RDX by Nitrolysis of Hexamethylenetetramine in Fluorous Media. *J. Hazard. Mater*. **2008**, *150*: 839-842.
[17] Richard, R. M.; Ball, D. W. B3LYP Calculations on the Thermodynamic Properties of a Series of Nitroxycubanes Having the Formula $C_8H_{8-x}(NO_3)_x$ (x=1–8). *J. Hazard. Mater*. **2009**, *164*: 1595-1600.
[18] Arabian, R.; Ramazani, A.; Mohtat, B.; Azizkhani, V.; Joo, S. W.; Rouhani, M. A Convenient and Efficient Protocol for the Synthesis of HBIW Catalyzed by Silica Nanoparticles under Ultrasound Irradiation. *J. Energ. Mater.* **2014**, *32*: 300-305.
[19] Bayat, Y.; Azizkhani, V. Synthesis of 4,10-Dinitro-2,6,8,12-tetraoxa-4,10-iazaisowurtzitane (TEX) Using Heteropolyacids as Efficient and Recyclable Heterogeneous Catalysts. *J. Energ. Mater.* **2012**, *30*: 209-219.
[20] Simpson, R. L.; Urtiew, P. A.; Ornellas, D. L.; Moody, G. L.; Scribner, K. J.; Hoffman, D. M. CL-20 Performance Exceeds that of HMX and its Sensitivity is Moderate. *Propellants Explos. Pyrotech.* **1997**, *2*: 249-255.
[21] Nielsen, A. T.; Nissan, R. A.; Vanderah, D. J.; Coon, C. L.; Gilardi, R. D.; George, C. F.; Flippen-Anderson, J. Polyazapolycyclics by Condensation of

Aldehydes with Amines, 2: Formation of 2,4,6,8,10,12-hexabenzyl-2,4,6,8,10,12-hexaazatetracyclo[5.5.0.05,9.03,11]dodecanes from Glyoxal and Benzylamines. *J. Org. Chem.* **1990**, *55*: 1459-1466.

[22] Sider, A. K.; Nirmala Sikder, B. R.; Gandhe, J. P.; Agrawal, S.; Haridwar, S. Hexanitrohexaazaisowurtzitane or CL-20 in India: Synthesis and Characterisation. *Defence Sci. J*. **2002**, *52*: 135-146.

[23] Suslick, K. S.; Casadonte, D. J.; Doktycz, S. J.; Shojate, R. The Effects of Ultrasound on Transition Metal Surfaces. *Solid State Ionics* **1988**, *26*: 176.

[24] Nabid, M. R.; Tabatabaei Rezaei, S. J.; Ghahremanzadeh, R.; Bazgir, A. An Efficient Ultrasound-promoted One Pot Synthesis of Spiroacenaphthylene Pyrazolotriazole and Pyrazolophthalazine Derivatives. *Ultrason. Sonochem.* **2010**, *17*: 159.

[25] Rouhani, M.; Ramazani, A.; Joo, S. W. Ultrasonics in Isocyanide-based Multicomponent Reactions: A New, Efficient and Fast Method for the Synthesis of Fully Substituted 1,3,4-Oxadiazole Derivatives under Ultrasound Irradiation. *Ultrason. Sonochem*. **2014**, *22*: 391-396.

[26] Rouhani, M.; Ramazani, A.; Joo, S. W. Novel, Fast and Efficient One-pot Sonochemical Synthesis of 2-Aryl-1,3,4-oxadiazoles. *Ultrason. Sonochem*. **2014**, *21*: 262-267.

[27] Tabatabaei Rezaei, S. J.; Bide, Y.; Nabid, M. R. An Efficient Ultrasound-promoted One Pot Synthesis of Spiroacenaphthylene Pyrazolotriazole and Pyrazolophthalazine Derivatives. *Tetrahedron Lett*. **2012**, *53*: 5123-5126.

[28] Shokrollahi, S.; Ramazani, A.; Tabatabaei Rezaei, S. J.; Mashhadi Malekzadeh, A.; Azimzadeh Asiabi, P.; Joo, S. W. Citric Acid as an Efficient and Green Catalyst for the Synthesis of Hexabenzyl Hexaazaisowurtzitane (HBIW). *Iranian J. Catal*. **2016**, *6*: 65-68.

[29] Tabatabaei Rezaei, S. J.; Nabid, M. R.; Yari, A.; Ng, S. W. Ultrasound-promoted Synthesis of Novel Spirooxindolo/Spiroacenaphthen Dicyano Pyrrolidines and Pyrrolizidines through Regioselective Azomethine Ylide Cycloaddition Reaction. *Ultrason. Sonochem*. **2011**, *18*: 49-53.

[30] Massart, R. Preparation of Aqueous Magnetic Liquids in Alkaline and Acidic Media. *IEEE Trans. Magn*. **1981**, *17*: 1247-1248.

[31] Adeli, M.; Mehdipour, E.; Bavadi, M. Encapsulation of Palladium Nanoparticles by Multiwall Carbon Nanotubes-graft-poly (Citric Acid) Hybrid Materials. *J. Appl. Poly. Sci*. **2010**, *116*: 2188-2196.

[32] Kayal, S.; Ramanujan, R. V. Doxorubicin Loaded PVA Coated Iron Oxide Nanoparticles for Targeted Drug Delivery. *Mater. Sci. Eng. C* **2010**, *30*: 484-490.

[33] Xiaolong, L.; Huan, L.; Guoqiang, L.; Ziwei, D.; Shuilin, W.; Penghui, L.; Haibo, X.; Paul, K.C.; Zushun, X. Magnetite-loaded Fuorine-containing Polymeric Micelles for Magnetic Resonance Imaging and Drug Delivery. *Biomaterials* **2012**, *33*: 3013-3024.

[34] Nabid, M. R.; Bide, Y.; Tabatabaei Rezaei, S. J. Pd Nanoparticles Immobilized on PAMAM-grafted MWCNTs Hybrid as New Recyclable Catalyst for Mizoraki-Heck Cross-coupling Reactions Materials. *Appl. Catal., A* **2011**, *406*: 124-132.